frontiers in Marine Science

ORIGINAL RESEARCH
published: 08 March 2022
doi: 10.3389/fmars.2022.856992

Hadal Biodiversity, Habitats and Potential Chemosynthesis in the Java Trench, Eastern Indian Ocean

Alan J. Jamieson[1,2], Heather A. Stewart[3,4], Johanna N. J. Weston[2], Patrick Lahey[5] and Victor L. Vescovo[6]*

[1] Minderoo-UWA Deep-Sea Research Centre, School of Biological Sciences, Oceans Institute, The University of Western Australia, Perth, WA, Australia, [2] School of Natural and Environmental Sciences, Newcastle University, Newcastle upon Tyne, United Kingdom, [3] British Geological Survey, Lyell Centre, Edinburgh, United Kingdom, [4] School of Energy, Geoscience, Infrastructure and Society, Institute of Life and Earth Sciences, Heriot-Watt University, Edinburgh, United Kingdom, [5] Triton Submarines LLC, Sebastian, FL, United States, [6] Caladan Oceanic LLC, Southlake, TX, United States

The Java Trench is the only subduction trench in the Indian Ocean that extends to the hadal zone (> 6,000 m water depth), and except for sevenbenthic trawls acquired around the 1950s, there has been little to no sampling at hadal depths undertaken since. In 2019, we undertook a 5-day expedition comprising a scientific dive using a full ocean depth-rated submersible, the DSV *Limiting Factor,* seven hadal-lander deployments, and high-resolution bathymetric survey. The submersible performed a video transect from the deepest point of the trench, up a 150 m high near-vertical escarpment located on the forearc, and then across a plateau at a depth of ∼7,050 m to make *in situ* observations of the habitat heterogeneity and biodiversity inhabiting these hadal depths. We found the Java Trench hadal community to be diverse and represented by 10 phyla, 21 classes, 34 orders and 55 families, with many new records and extensions in either depth or geographic range, including a rare encounter of a hadal ascidian. The submersible transect revealed six habitats spanning the terrain. The deepest trench axis comprised fine-grained sediments dominated by holothurians, whereas evidence of active rock slope failure and associated talus deposits were prevalent in near-vertical and vertical sections of the escarpment. Sediment pockets and sediment pouring down the steep wall in "chutes" were commonly observed. The slope terrain was dominated by two species in the order Actiniaria and an asteroid, as well as 36 instances of orange, yellow, and white bacterial mats, likely exploiting discontinuities in the exposed bedrock, that may indicate a prevalence of chemosynthetic input into this hadal ecosystem. Near the top of the escarpment was an overhang populated by > 100 hexactinellid (glass) sponges. The substrate of the plateau returned to fine-grained sediment, but with a decreased density and diversity of epifauna relative to the trench floor. By providing the first visual insights of the hadal habitats and fauna of the Java Trench, this study highlights how the habitat heterogeneity influences patchy species distributions, and the great benefit of using a hadal-rated exploratory vehicle to comprehensively assess the biodiversity of hadal ecosystems.

Keywords: Deep Sea, subduction trench, fore arc, epifauna, bacterial mats, submersible

OPEN ACCESS

Edited by:
Daniela Zeppilli, Institut Français de Recherche pour l'Exploitation de la Mer (IFREMER), France

Reviewed by:
Tomo Kitahashi, Japan Agency for Marine-Earth Science and Technology (JAMSTEC), Japan
Saskia Brix, Senckenberg Museum, Germany

****Correspondence:***
Alan J. Jamieson
alan.j.jamieson@uwa.edu.au

Specialty section:
This article was submitted to Deep-Sea Environments and Ecology, a section of the journal Frontiers in Marine Science

Received: *18 January 2022*
Accepted: *10 February 2022*
Published: *08 March 2022*

Citation:
Jamieson AJ, Stewart HA, Weston JNJ, Lahey P and Vescovo VL (2022) Hadal Biodiversity, Habitats and Potential Chemosynthesis in the Java Trench, Eastern Indian Ocean. Front. Mar. Sci. 9:856992. doi: 10.3389/fmars.2022.856992

INTRODUCTION

The Indian Ocean is the world's third largest ocean spanning 70,560,000 km^2, accounting for 19.5 and 19.8% of the global ocean area and volume, respectively (Eakins and Sharman, 2020). It is the least understood of the five oceans (Stefanoudis et al., 2020), as historically it was largely scientifically neglected up to the late-1950s (Rogers, 2016). The Indian Ocean is geomorphologically complex, hosting subduction trenches, seamounts, ridges, plateaus, coral atolls, fracture zones and hydrothermal vents. The Indian Ocean is largely bounded by canyon-incised continental slopes (Daniell et al., 2010; Harris et al., 2014) that in places can plunge from the coast to > 7,000 m deep (Stewart and Jamieson, 2019). Numerous expeditions and institutional efforts in the last two centuries have contributed greatly to our knowledge of coastal marine biodiversity within the Indian Ocean (Wafar et al., 2011). However, assessments of deep benthic fauna at abyssal depths of the Indian Ocean are infrequent and rarely exceed 5,000 m (e.g., Parulekar et al., 1982; Janßen et al., 2000; Pavithran et al., 2009; Wolff et al., 2011), or cross the abyssal-hadal boundary (Weston et al., 2020, 2021).

Contemporary marine science has acknowledged the global importance of understanding Indian Ocean biodiversity for habitat management and are focussing efforts on, for example, coral reefs (Sheppard, 1998; Wafar et al., 2011; McClanahan and Muthiga, 2016) and seamount associated pelagic communities (Rogers, 2016; Rogers et al., 2017), typically in the upper 3,000 m. However, the average depth of the Indian Ocean is 3,741 m (Eakins and Sharman, 2020) and hosts vast areas, particularly in the East Indian Ocean, that exceed 6,000 m (e.g., the Wharton Basin, Java Trench, and the Wallaby-Zenith and Diamantina fracture zones; Jamieson, 2015; Stewart and Jamieson, 2019; Bongiovanni et al., 2021; Weston et al., 2021).

The geomorphological complexity of the East Indian Ocean has recently been highlighted by the high-resolution and large-scale multibeam mapping that has been acquired during the search for the lost Malaysian Airliner MH370, particularly the Diamantina Fracture Zone (Smith and Marks, 2014; Picard et al., 2018; Wölfl et al., 2019). Furthermore, the exact depth of other features, for example the Wallaby-Zenith Fracture Zone, has been substantially corrected from the original satellite altimetry-derived to new multibeam echosounder-derived bathymetry (Weston et al., 2021). In fact, during the search for the deepest point in the Indian Ocean for the 2019 *Five Deeps Expedition* (Jamieson, 2020) it was not clear if the Java Trench or Diamantina Fracture Zone was deeper (Stewart and Jamieson, 2019). After conducting multibeam transects at both features, the *Five Deeps Expedition* demonstrated that the Java Trench holds the deepest point in the Indian Ocean, with of depth of 7,187 ± 13 m at an unnamed deep at 11.129° S/114.942° E (Bongiovanni et al., 2021).

The Java Trench, also known as the Sunda Trench (e.g., Omura et al., 2017), is located south and west of the islands of Java and Sumatra. The Java Trench is ∼3,200 km in length and is the only subduction trench to extend to the hadal zone in the Indian Ocean, making it a geographically isolated hadal ecosystem (Stewart and Jamieson, 2018). Very little biological sampling occurred in the Java Trench or surrounding hadal features for nearly six decades since the RV *Galathea* and RV *Vitjaz* expeditions of the 1950s (Belyaev, 1989). However, the Wallaby-Zenith Fracture Zone was visited by the RV *Sonne* in 2017, as was the Java Trench in 2019 by the DSSV *Pressure Drop*. Those expeditions produced the first accounts of the scavenging amphipods, fish, decapods, octopods, and gelatinous organisms from those areas (Jamieson and Vecchione, 2020; Jamieson et al., 2021; Jamieson and Linley, 2021; Swan et al., 2021; Weston et al., 2021, respectively). The studies were all based upon mobile fauna observed by baited lander, or accompanying baited traps, which cannot resolve distribution patterns of epifauna, habitat heterogeneity or the presence of enigmatic systems such as chemosynthetic bacterial mats.

The Danish *Galathea* Expedition (1950–1952), sampled the deep Indian Ocean with trawls and dredges 50 times to depths exceeding 3,700 m (Belyaev, 1989). However, only three of these 50 trawls succeeded in obtaining biological specimens. These three sites were in the Java Trench (6,730, 6,900–7,000, and 7,160 m deep). Eight years later the former-Soviet Union expedition on the RV *Vityaz* obtained the only other known samples from the Java Trench, with four trawls and two dredges between 6,433 and 7,060 m deep (Belyaev, 1989). Combined, these campaigns collected 43 species with represented 35 families, 26 orders, and 16 classes in nine phyla. Annelids were the most common, with 12 species from eight families, and then, crustaceans with 10 species in nine families, most of which four were isopods. Of the echinoderms, they found four types of holothurians (three *Elpidia* and one Apodid), and single species of echinoid, asteroid, and ophiuroid.

Chemosynthesis has been speculated to occur along the forearcs of subduction trenches (Blankenship-Williams and Levin, 2009). Cold seeps have been found in the Japan Trench at 6,437 and 7,326 m (Fujikura et al., 1999; Fujiwara et al., 2001), and in the Mariana Trench a serpentinite-hosted ecosystem, the Shinkai Seep Field (SSF), is known from 7,500 m (Ohara et al., 2012; Okumura et al., 2016). Hand et al. (2020) speculated that filaments attached to the talus and outcrop at 10,677 m in *Sirena Deep* in the Mariana Trench may be chemolithoautrophic microbial mats. These cold seeps and putative microbial mats are located at the trench forearcs. Tokuda et al. (2020) found that amphipods from the Mariana and Kermadec trenches consumed, amongst other sources, possible seep-derived organic material. Together, these studies provide indirect evidence that chemosynthesis contributes to the energy budget of the hadal community. However, identification of chemosynthetic habitats is difficult due to the technical challenges of operating at great depth and the complexity of forearc topographies.

The DSSV *Pressure Drop* expedition undertook a scientific submersible dive to the base of the forearc (7,180 m) of the Java Trench, aimed at assessing the epifaunal communities and habitat heterogeneity from the trench floor to a near-vertical slope of the forearc. Additionally, signs of chemosynthetic processes were assessed. This work aims to provide the first visual insight into the habitats and fauna of the hadal Indian Ocean.

MATERIALS AND METHODS

Sampling Equipment

To identify the locality of the deepest point, the Java Trench was surveyed with a high-precision, full ocean depth rated 1° x 2° Kongsberg EM 124 multibeam echosounder (MBES) on a hull-mounted gondola fixed ∼20 m from the ship's bow (Bongiovanni et al., 2021). The MBES had a nominal frequency of 12 kHz, with an operating frequency of 10.5–13.5 kHz. Lockheed Martin/Sippican T-5 expendable bathythermographs (XBTs), depth and temperature accuracies of + 2% and + 0.1°C, respectively, were used to collect depth and temperature data in the upper 1,800 m of water column. In addition to the XBT data, the submersible and supporting landers were each equipped with CTD probes (SBE 49 FastCAT; SeaBird Electronics, Bellevue, WA) that during both the descent and ascent recorded salinity, temperature and depth profiles. These data were used to calculate full-ocean sound velocity profiles for the EM 124 MBES and to validate the submersible dive depths.

The submersible used was the Deep Submergence Vehicle (DSV) *Limiting Factor* (Triton 36,000/2, Triton Submarines LLC, United States; Jamieson et al., 2019; **Figure 1**), rated to full-ocean depth and capable of carrying a pilot and a scientific observer. The seafloor and faunal imagery was recorded using four externally mounted HD video cameras (IP Multi SeaCam 3105; Deep Sea Power and Light, San Diego, CA), illuminated by ten 15,500 lumen LED lights (LED-1153-A3-SUS; Teledyne Bowtech, Aberdeen, United Kingdom). The submersible was piloted manually and aimed to keep a steady altitude of 2 m off the seafloor. The system did not have an accurate underwater navigation system, and thus continuous positioning data was not recorded. Therefore, locations are estimated based on depth from twin CTD probes (SBE 49 FastCAT, SeaBird Electronics, US), with reference to rendezvous positions with three free-fall autonomous landers (hadal-landers), *Skaff*, *Flere,* and *Closp,* that were static and triangulated acoustically from the surface vessel DSSV *Pressure Drop* and support boat *Learned Response*, prior to the submersible dive.

In addition to providing fixed navigation points for the submersible, the three identical hadal-landers were also used to deliver baited cameras and CTDs to the study sites (Jamieson et al., 2019). These landers each had a high-definition video camera (IP Multi SeaCam 3105; Deep Sea Power and Light, San Diego, CA) positioned horizontally, 30 cm off the seafloor, with the field-of-view centered on the bait that protruded 1 m from the lander and supported the bait (mackerel; *Scomber* sp.). The cameras were set to record continuously with scene illumination provided by single LED lamps (LED SeaLite; Deep Sea Power and Light, San Diego, CA). These data were used to further assess the seafloor habitat substrate and provide additional information on local biodiversity.

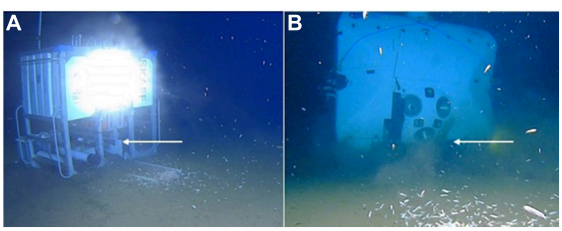

FIGURE 1 | The hadal-lander lander *Skaff* **(A)** and the submersible DSV *Limiting Factor* **(B)** imaging each other at the deepest point in the Indian Ocean, Java Trench, 7,192 m. Arrows indicate the location of the high-definition video cameras.

Study Site

The Java Trench is formed as the Indo-Australian Plate subducts beneath the Eurasian Plate, at a rate of 73 ± 0.8 mm yr^{-1} decreasing in velocity eastward to 60 ± 0.4 mm yr^{-1} (DeMets et al., 2010; **Figure 2**). The ∼3,200 km long trench axis descends to depths of > 7,100 m (Stewart and Jamieson, 2019), culminating in the deepest depression at 11.129° S/114.942° E at a depth of 7,192 ± 5 m (Bongiovanni et al., 2021). The area of the trench > 6,000 m is estimated to be 22,689 km^2 (Stewart and Jamieson, 2018). Along with the neighboring Banda Trench (or Weber Basin), the Java Trench underlies a highly productive biogeochemical province, the Sunda-Arafura Sea Coastal province (SUND), with an estimated primary production rate of 328 g C m^{-2} yr^{-1} (Longhurst, 2007).

Operations

The 5-day diving operation consisted of seven deployments of the hadal-landers two dives with the submersible, of which one was for scientific research (**Table 1**). Prior to the dive, the hadal-lander *Skaff* was deployed to the deepest point to derive seawater density in order to properly ballast the submersible. The scientific dive described in this study, was a ∼2.5 h transect from the deepest point of the trench and heading northwest up a steep, near-vertical slope ∼150 m high before crossing a relatively flat plateau to cover as many potentially different habitats as possible in one dive. During this dive the seafloor was visible for 1 h and 56 min. The hadal-landers were deployed to sample discreet depth zones as well as the start and end of submersible transects and were selected based on the high-resolution bathymetric survey data. The submersible transect was performed at a relatively constant speed and altitude, but as the submersible did not have an auto-pilot feature the speed and altitude varied throughout the dive. We estimate a mean speed of 20 $m.min^{-1}$ on flat terrain with a horizontal field of view of the camera of 3 m, and 10 $m.min^{-1}$ on vertical terrains, although in the latter, navigating and obstacle avoidance during the vertical ascent resulted in a highly variable speed. We estimate the distance traversed on the trench floor was 0.4 km and on the plateau was 0.9 km. While the height of the near-vertical slope was 150 m, due to periods of lateral survey and intense obstacle avoidance it is estimated the submersible track length was ∼500 m from the bottom to the top of the slope.

Species Density Estimates

As the submersible lacked real-time positioning or recording of over ground speed, the density of benthic organisms was only

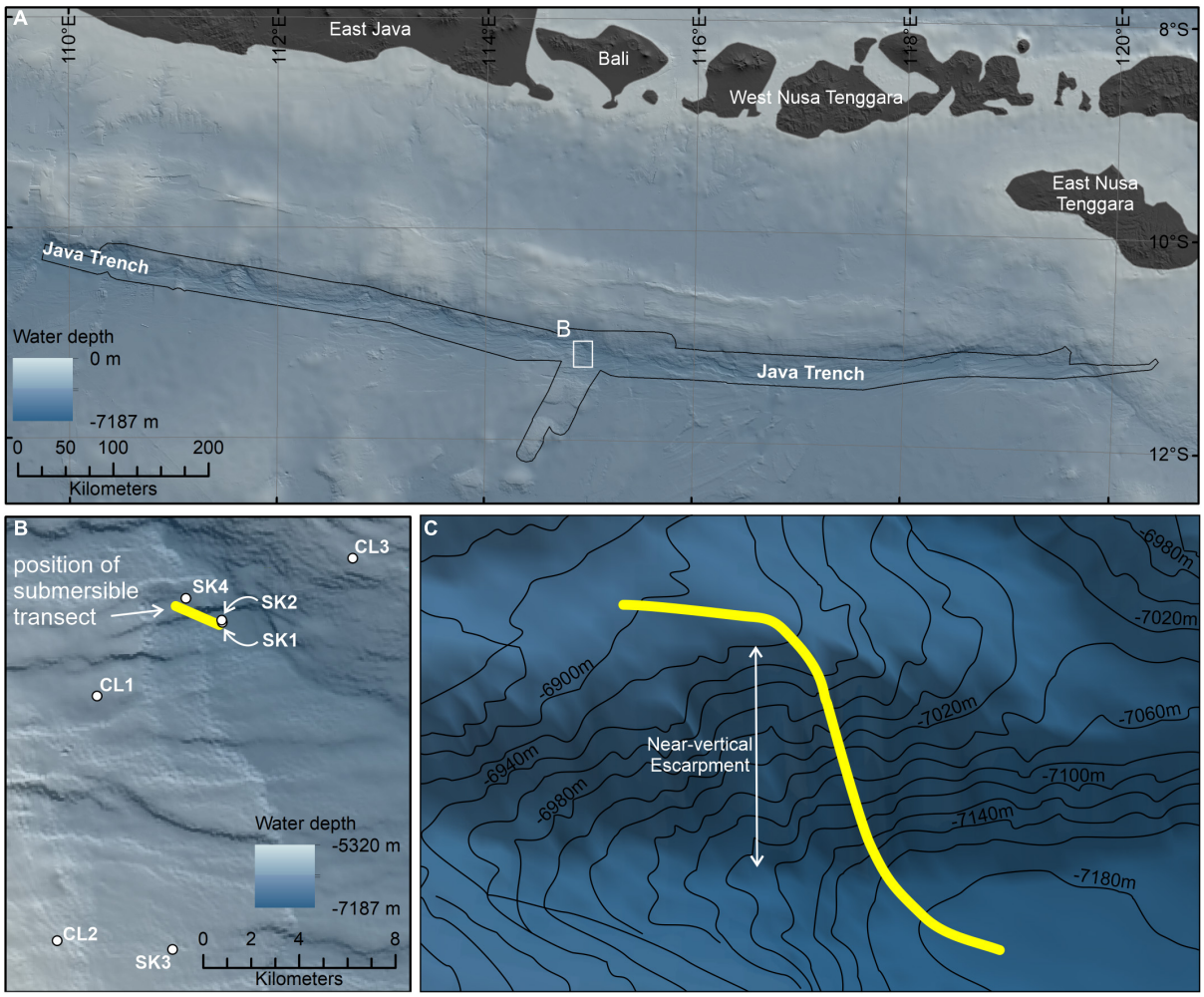

FIGURE 2 | (A) The study area within the Java Trench, Indian Ocean, with the **(B)** seven hadal-lander deployments (white circles) and submersible dive transect starting at the deepest point of the trench (yellow line). **(C)** Three-dimensional representation of the approximate submersible dive transect up the near-vertical fault escarpment on the forearc. Location of inset **(B)** delineated by the white box in **(A)**. Extent of Five Deeps Expedition multibeam bathymetry data (Bongiovanni et al., 2021) delineated by the black outline in **(A)** and displayed in **(B,C)**. Regional elevation data in **(A)** sourced from the GEBCO Compilation Group (2021). The figure was created in ESRI ArcGIS v10.7.

TABLE 1 | Deployment details of the lander and submersible dives including bottom time, bottom temperature, and salinity.

Station	Date	Year	Gear	Latitude	Longitude	Depth (m)	Bottom time	Temp. (°C)	Salinity
JAV_SK1_7200	02-Apr	2019	SKAFF	−11.1289	114.9418	7,168	4 h 00 min	1.54	34.7
JAV_SK2_7200	05-Apr	2019	SKAFF	−11.1283	114.9416	7,176	6 h 37 min	1.54	34.7
JAV_CL1_6500	05-Apr	2019	CLOSP	−11.1566	114.8950	6,439	6 h 57 min	1.43	34.7
JAV_CL2_6200	06-Apr	2019	CLOSP	−11.2483	114.8800	5,760	6 h 41 min	1.34	34.7
JAV_SK3_5700	06-Apr	2019	SKAFF	−11.2516	114.9233	6,146	6 h 6 min	1.39	34.7
JAV_CL3_6700	07-Apr	2019	CLOSP	−11.1050	114.9906	6,737	3 h 47 min	1.47	34.7
JAV_SK4_6900	07-Apr	2019	SKAFF	−11.1200	114.9283	6,957	4 h 59 min	1.51	34.7
JAV_LF_SCI	07-Apr	2019	LF	−11.1218	114.9262	7,180	1 h 56 min*	1.54	34.7

*LF, DSV Limiting Factor (submersible). * indicates bottom time where seafloor was visible. For location see **Figure 2B** noting the corresponding label comprises only the central part of the station name.*

estimated, and should be taken as indicative and not quantitative. On flat terrain, the density of common species (Ind.km^{-2}) was calculated assuming the 3 m wide field of view at a speed of 20 m.min^{-1}. On vertical ascents, the field of view remained ∼3 m but the distance traveled used was the height of the ascent at the slower speed of 10 m.min^{-1}.

RESULTS

Environmental

Beyond 2,000 m deep, the salinity of the Java Trench remained constant at 34.7 to the maximum water depths encountered (**Figure 3**). The temperature decreased from 30°C at the surface to ∼5°C at 1,000 m, 2.5°C at 2,000 m reaching a temperature minimum of 1.18°C at ∼4,250 m. Thereafter, the temperature increased to 1.54°C at the deepest point (7,192 m), consistent with adiabatic heating. The near-bottom temperatures of the hadal-lander sites increased to 1.34°C at the shallowest site (5,760 m), and 1.54°C at the deepest two sites (**Table 1**).

Geology and Habitat-Heterogeneity

The hadal-landers showed that the substrates on the slopes of the Java Trench were comprised of poorly sorted substrate, featuring a fine-grained matrix with irregularly shaped gravel and cobble sized material (**Figure 4**). The sediment did, however, get progressively softer with depth as indicated by the position of the bait arm on the landers. From 5,760 to 6,737 m, the bait arm settled ∼3 cm above the seafloor, whereas from 6,957 to 7,176 m, the bait arm was either partially embedded or completely buried in sediment, as in the case of the 7,168 m site. No obvious current indicators such as scour, lineations or sediment tails are observed from the lander footage.

The submersible transect revealed six broad habitat classes (**Table 2** and **Figure 5**). Beginning at the deepest point of the Java Trench, observed substrates comprised fine-grained sediment (Habitat 1) with abundant lebenspurren and no obvious indications of bottom-current activity (see "trench axis" **Figure 4**). Overall the ∼150 m high near-vertical escarpment, or wall (**Figure 2C**), comprises sections of exposed bedrock with associated talus deposits at the base of those terraces. Observations from the submersible footage suggests that vertical cliff sections and extensive talus deposits are ubiquitous in the lower slope habitat (Habitat 3 and 4, see "lower slope" **Figure 4**), compared to the upper slope where a decrease in overall slope angle results in comparatively shorter vertical sections of bedrock outcrop, more localized talus deposits and larger fine-grained sediment pockets (Habitat 5 and 6, see "upper slope" **Figure 4**). The submersible transect ended on a relatively flat plateau also comprising fine-grained sediments (Habitat 1, see "plateau" **Figure 4**) with conspicuously fewer lebenspurren observed than the trench axis.

Evidence of active erosion was first encountered at the base of the near-vertical fault escarpment, characterized by angular talus blocks and rubble piles (**Figure 6A**). Larger talus deposits were observed 34 times during the transect up the ∼150 m escarpment including tabular-shaped boulders (**Figure 6B**) likely indicative of a short transport distance. Block failure where discontinuity orientation is likely a controlling factor, creating planes of structural weakness within the rock mass, has resulted in repeated rock slope failure (**Figures 6C–I**). Although the exact dip and strike of joint sets cannot be ascertained from the submersible footage, it appears that they dip out of the face of the rock wall (e.g., **Figures 6F,H,I**) with wedge block failures exposing discontinuous bedrock ledges exhibiting "saw tooth" profiles (**Figures 6C–E**). The resultant angular detachment blocks form the localized talus deposits described herein. From the submersible footage alone, it is not possible to conclusively state whether the talus blocks were deposited during one catastrophic failure event or are the result of continued (and possibly ongoing) individual failure incidents.

Toward the top of the slope, as it began to plateau onto a flatter plain (**Figure 5B**), the submersible inadvertently maneuvered

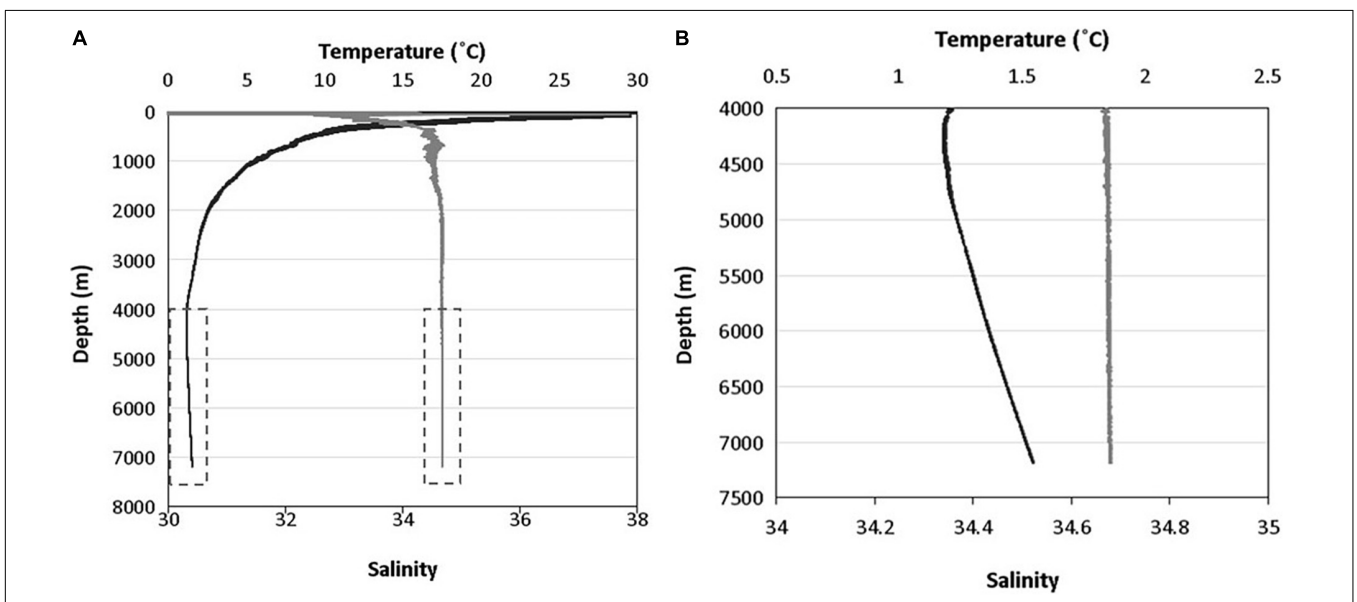

FIGURE 3 | Temperature (black), salinity (gray) with depth profiles from the surface to deepest point in the Java Trench **(A)**, and magnified between 4,000 and 7,500 m to show adiabatic heating **(B)**. The dashed boxes in **(A)** represent the data shown in **(B)**.

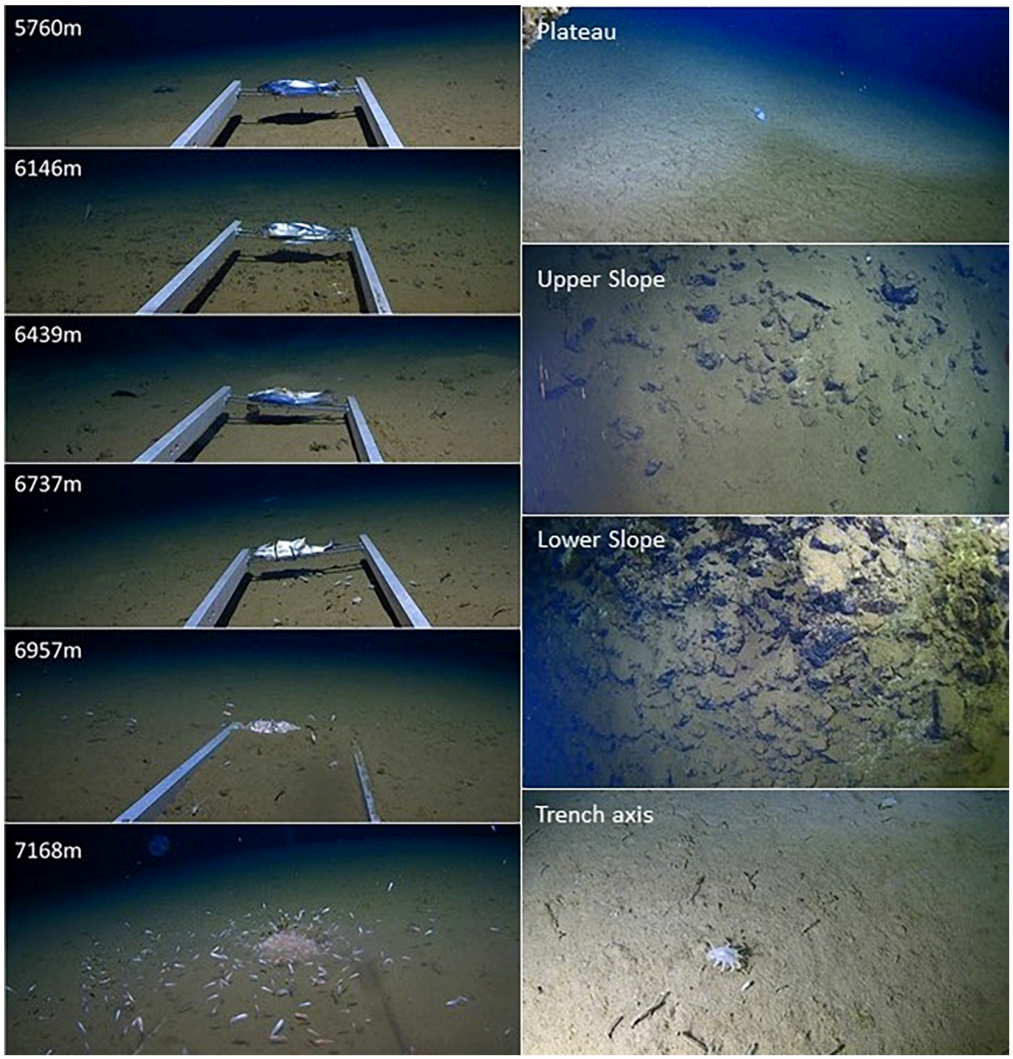

FIGURE 4 | Seafloor substrates as observed by the hadal-lander at increasing depths from 5,760 to 7,168 m (left panels). Typical substrates as observed by the submersible on the plateau, upper and lower slope, and the trench axis (right panels).

underneath an overhang, a few meters deep, recessed into the otherwise steep incline with associated talus deposit clearly visible (**Figure 6G**). At the very top of the slope, there was a broad reduction in slope angle of the overall escarpment resulting in smaller bedrock exposures and a reduction in the amount of talus deposited locally. Observation suggests a change in the structure of the bedrock resulting in thinner stratification of exposed surfaces with burrows in softer layers and possible chemosynthetic deposits following the bedrock structure (**Figure 7F**).

Potential Chemosynthetic Bacterial Mats

During the ascent of the slope, there were 36 observations of potential chemosynthetic deposits (**Figure 7**). These deposits were orange, yellow, and white in color and exploited structural weaknesses in the bedrock and around talus blocks. No obvious metazoan organisms were associated with these deposits.

Anthropogenic and Terrestrial Signatures

Litter was seen through the trench axis, slope, and plateau. Notably, between the 210 m traveled from the trench axis to the base of the slope, 13 items were seen. The items seen ranged from floating plastic bags to unidentified plastic, some possibly metal, manmade objects embedded on the sediment. Similar items were seen on the plateau and slope with reducing density, respectively. On the trench axis, two wooden branches and half a coconut shell were observed on the seafloor.

Benthic Megafauna

The rear of the recess in the overhang was populated by hexactinellid sponges, possibly in the subclass Hexasterophora (**Figure 8**). The hexactinellid sponges numbered more than 100 individuals, but their spatial extent could not be determined.

As the submersible traversed the fine-grained trench floor during the first 20 min of the dive, four holothurian species (order

TABLE 2 | Seafloor characterization of dominant habitats as shown in **Figure 5A**.

Habitat	Description	Terrain
1	Fine-grained sediment.	Trench axis, Plateau
2	Angular talus deposit of mixed sizes, including boulders, with a veneer of fine-grained sediment found at base of bedrock terraces/cliffs.	Lower slope, Upper slope
3	Angular talus deposit with a veneer of fine-grained sediment.	Lower slope
4	Near vertical exposures of bedrock separated by areas of ponded sediment and talus deposits.	Lower slope, Upper slope
5	Bedrock cropping out at seabed, some talus deposits. Veneer of fine-grained sediment. Putative chemosynthetic deposits becoming more prevalent.	Upper slope
6	Overall reduction in general slope angle with smaller exposures of thinly stratified bedrock with frequent observed putative chemosynthetic deposits and some potential burrows in softer strata. Larger areas of fine-grained sediment blanketing the sea floor.	Upper slope
PV	Poor visibility.	Plateau

Elasipodida) were seen (**Figures 9A–D**, **10A,B**). The two most abundant species were *Amperima* cf. *naresi* (Théel, 1882) and *Elpidia* cf. *sundensis* Hansen, 1956. The estimated density of *A*.cf. *naresi* at the trench axis was 7.0 Ind.km^{-2} whereas *E.* cf. *sundensis* was 14 Ind.km^{-2}. A third species, *Psychropotes* sp., was seen three times within the trench axis (2.6 Ind.km^{-2}) (**Figure 9D**). On the upper plateau, a single *Enypniastes* sp. was seen swimming near the seafloor (**Figure 9C**) and one individual of *A.* cf. *naresi* (**Figure 9A**). Apart from these two individuals, no holothurians were observed on the plateau or the slope.

Three classes of echinoderms were observed, namely ophiuroids or brittle stars (Ophiuroidea), asteroids or sea stars (Asteroidea), and crinoids or feather stars (Crinoidea). Ninety-eight unidentified ophiuroids (*Ophiuroid* sp. 1) were seen on the seafloor of the trench axis (**Figure 9J**), giving an estimated density of 86 Ind.km^{-2}. The ophiuroids were distributed with increasing density with proximity to the base of the slope. On the slope itself, they were seen in a small clusters associated with fine grained sediment pockets observed among the talus and bedrock outcrops, but were generally not present on the slope. Across the plateau, the ophiuroid density decreased to 21.9 Ind.km^{-2}. Two individuals of a second species (*ophiuroid* sp. 2) were observed at the hadal-lander site at 6,146 m depth (**Figure 9Q**). No asteroids, *Hymenaster* sp., were observed within the trench axis or on the plateau (**Figure 9I**), but rather were only found attached to talus blocks on the near-vertical escarpment (**Figure 10C**). Thirty-two asteroids were seen on the slope, an estimated density of ∼53.3 Ind.km^{-2}. Fragile and almost transparent crinoids of an unknown family were occasionally seen within talus deposits (**Figure 9K**). Another species of crinoid, resembling the family Bathycrinidae, was seen at 6,439 m by the hadal-lander (**Figure 9M**).

Two unidentified species of sea anemones (Actiniaria) were seen attached to variously sized talus blocks present only on the near-vertical escarpment. The first observed anemone species, aff. *Galatheanthemum* (Galatheanthemidae), was seen 55 times (density estimate of 91.7 Ind.km^{-2}), with the highest density toward the base of the slope (**Figures 9F**, **10D**). A second species, aff. *Bathyphellia* (Bathyphelliidae), was observed 140 times during the ∼150 m ascent up the slope, with an estimated density of 233.3 Ind.km^{-2} (**Figure 9G**).

Several polychaetes belonging to the family Polynoidae, aff. *Macellicephaloides,* were seen within the fine-grained sediment of the trench axis (**Figure 9L**).

The hadal-landers also recorded the peracarid crustacean orders Isopoda, Mysida and Amphipoda. Two munnopsid isopods (Munnopsidae) were seen near the base of the slope, and five were seen on the plateau (**Figure 9E**). Individuals were also recorded present at 6,439, 6,737, and 6,957 m by the hadal-landers. Mysida and Amphipoda, were seen swimming and feeding on the bait. The mysid, aff. *Amblyops* sp., was seen at stations deployed at 5,760 and 7,176 m depth (**Figure 9R**). Four medium to large-sized species of amphipods were identifiable, specifically *Alicella gigantea* Chevreux, 1899 between 6,957 and 7,176 m (**Figure 9N**), aff. *Princaxelia* (Pardaliscidae) between 5,760 and 6,957 m (**Figure 9S**), *Bathycallisoma schellenbergi* (Birstein and Vinogradov, 1958) between 6,957 and 7,176 m (**Figure 9O**), and an unidentified species in the family Stegocephalidae between 6,957 and 7,176 m (**Figure 9P**) depth.

Perhaps the most obscure observation was of a stalked ascidian tunicate, aff. *Culeolus* sp., that had become uncoupled from the seafloor, and drifted passed the hadal-lander at 6,430 m depth (**Figure 9T**).

The landers also recorded some additional mobile fauna that are presented in separate studies, specifically decapods (Swan et al., 2021), cirrate octopus *Grimpoteuthis* sp. (Jamieson and Vecchione, 2020), larvaceans (Jamieson and Linley, 2021), and fish comprising seven Ophidiidae species, one Ateleopodidae species and one liparid species (Jamieson et al., 2021). Only the liparids were seen during the submersible dive with one individual at the base of the slope, one individual near the top of the slope, and four individuals on the plateau (**Figure 9H**).

DISCUSSION

The Java Trench has gone largely unexplored, except for brief trawl surveys in the 1950s, it is not surprising that any new study will immediately produce many new records and significant extensions in either depth or geographic range across many species of benthic organisms. For example, on the same 5-day expedition, the first hadal cephalopods were found (Jamieson and Vecchione, 2020), as were the deepest Indian Ocean decapods (Swan et al., 2021), the deepest larvaceans (Jamieson and Linley, 2021) and multiple new species records of hadal fish were found, and mostly all new for the Indian Ocean (Jamieson et al., 2021). Indeed, the snailfish (Liparidae) reported here was the first hadal snailfish record from the Indian Ocean. Similarly, this expedition provided the first record of a hadal ascidian and hexactinellid sponges (Jamieson, 2015) and putative evidence for chemosynthesis. Interestingly, the hadal hexactinellid sponges found inside an overhang, a setting comparable to the caves they are known from at littoral depths (Vacelet et al., 1994). These

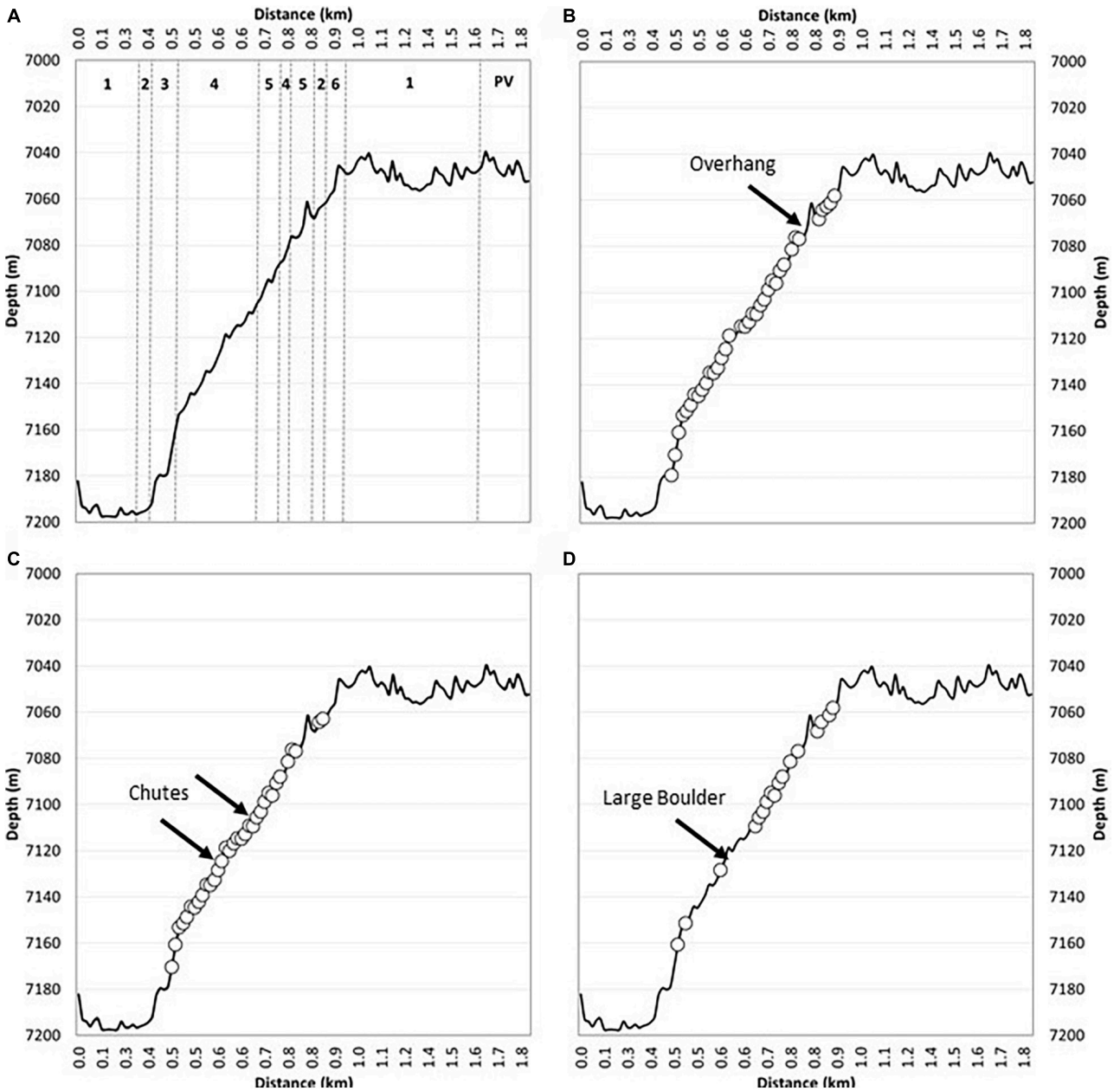

FIGURE 5 | Habitat characteristics of the submersible transect of the near-vertical forearc at 7,180–7,050 m. Depth profile of the submersible transect against estimated horizontal distance with the six habitat types described in **Table 2 (A)**. Location of observed chemosynthetic deposits (e.g., **Figure 7**) (circles) and the overhang (**Figure 6G**) labeled **(B)**. Areas of observed talus deposits (circles) with large sediment chutes indicated (note smaller chutes were frequently observed) **(C)**. Larger bedrock terraces and cliffs (circles) with location of large boulder (**Figure 6B**) labeled **(D)**.

accolades simply serve as indicators of how little the deep Indian Ocean has been explored.

Diverse Hadal Community

The Java Trench is also unique in that it is the only large, hadal subduction trench in the Indian Ocean. The geographically closest hadal trench is the Banda Trench (or Weber Basin), however, these two trenches are separated by the Savu and Timor seas and the Islands of eastern Indonesia and Timor which form physical barriers to connectivity. While there are vast expanses of seafloor between 6,000 and 6,500 m deep to the south of the Java Trench, within the Wharton Basin and the Wallaby-Zenith and Diamantina fracture zones, overall the hadal communities are largely restricted to the East Indian Ocean, separated from the latitudinally expansive trench systems of the Western Pacific by Indonesia and the Australian continent. Nonetheless, the benthic fauna of the Java Trench exhibit many similarities to those known from other trenches, such as the prevalence of the

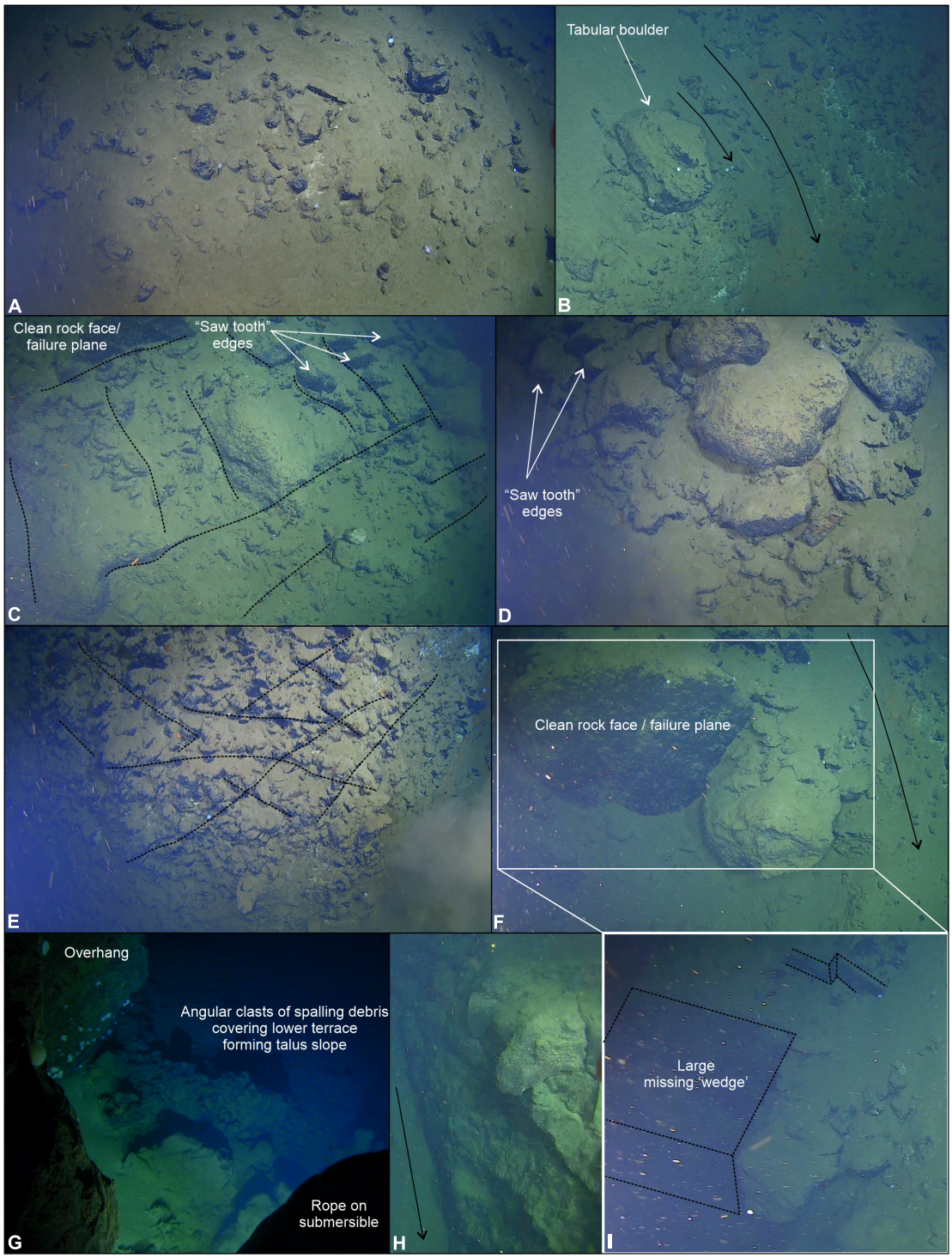

FIGURE 6 | Bedrock outcrop and active erosion observed over the near-vertical fault escarpment. **(A)** Angular talus blocks and rubbles piles observed at the very base of the escarpment. **(B)** Large tabular boulder > 1 m in diameter likely transported a short distance from an escarpment further upslope, smaller talus fragments are visible. **(C)** Orientation of discontinuities (e.g., joint sets) form planes of weakness (black dotted lines) resulting in rock slope failure (e.g., clean failure plane) and saw tooth profile along ledge edges. **(D)** Bedrock exposed in near-vertical section of the escarpment with a veneer of fine-grained sediments. **(E)** Heavily fractured and jointed bedrock resulting in area of abundant saw tooth edged ledges. **(F)** Wedge block failure > 2 m^3. **(G)** Overhang near the top of the ~150 m high escarpment showing clean failure plane and talus deposit beneath the cliff. **(H)** Example of jointing visible within the rock face. **(I)** Alternative view of the wedge failure shown in **(F)**. Black arrows indicate small sediment chutes forming conduits for sediment to pour down the steep walls of the trench.

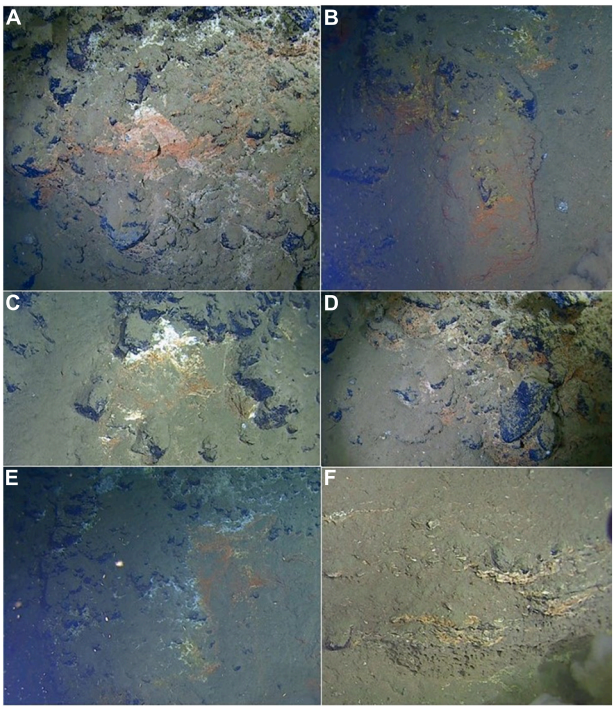

FIGURE 7 | Examples of brightly colored putative chemosynthetic deposits observed by submersible on the ∼150 m high near-vertical wall (7,180–7,050 m water depth), north slope of the Java Trench. Putative chemosynthetic deposits exploiting planes of weakness in the host rock **(A–E)**. Thinly stratified strata with potential chemosynthetic deposits following the bedrock structure, burrows are observed in the pooled sediment below the bedrock outcrops **(F)**.

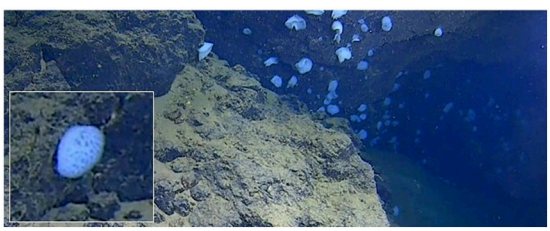

FIGURE 8 | The recess on the upper slope, inhabited by > 100 hexactinellid sponges. Inset: Individual magnified x3.

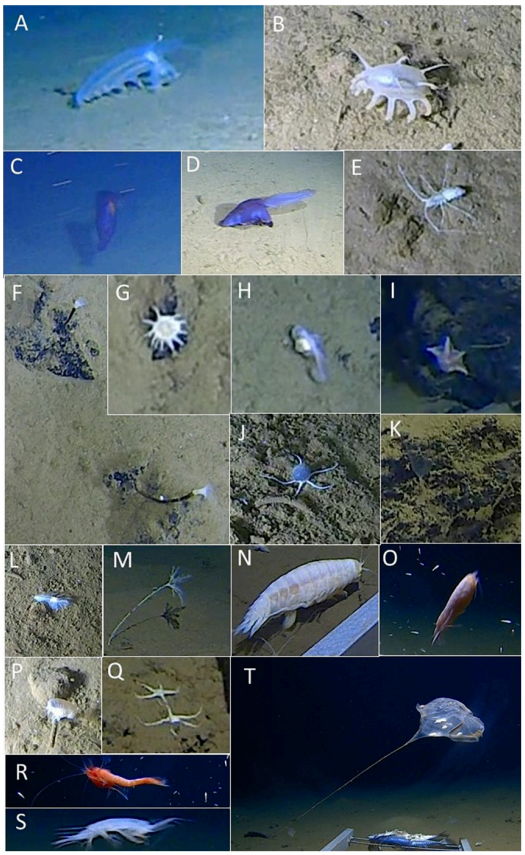

FIGURE 9 | Benthic fauna of the Java Trench. Holothurians: **(A)** *Amperima* cf. *naresi,* **(B)** *Elpidia* cf. *sundensis*, **(C)** *Enypniastes* sp., **(D)** *Psychropotes* sp., and **(D)** *Elpidia* cf. *sundensis*. **(E)** Munnopsid isopod. Actiniaria: **(F)** aff. *Galatheanthemum* and **(G)** aff. *Bathyphellia*. **(H)** Snailfish. Echinoderms: **(I)** the asteroid *Hymenaster* sp., **(J)** unidentified *Ophiuroid* sp. 1, **(K)** fragile, semi-transparent Crinoids?, **(M)** unidentified crinoid, and **(Q)** unidentified *Ophiuroid* sp. 2. **(L)** The polynoid polychaete aff. *Macellicephaloides.* Amphipods: **(N)** the "supergiant" *Alicella gigantea*, **(O)** *Bathycallisoma schellenbergi*, **(P)** the unidentified Stegocephalidae species, and **(S)** the pardaliscid aff. *Princaxelia*. **(R)** The Mysid *Amblyops* sp. **(T)** The stalked ascidian, aff. *Culeolus* sp. Images **(A–L)** were captured by the submersible, and imaged **(M–T)** observed by the hadal-landers.

holothurians within the trench axis (Wolff, 1960), particularly of the family Elpididae (Jamieson et al., 2011) and the presence of crinoids (Oji et al., 2009), polynoid polychaetes (Paterson et al., 2009), munnopsid isopods (Jamieson et al., 2012a), amphipods of the Scopelocheridae, Alicellidae, and Pardaliscidae families (Jamieson et al., 2012b, 2013; Lacey et al., 2018; respectively). *Bathycallisoma schellenbergi* has been known from the Java Trench as it was sampled by historical expeditions and also from hadal depths of the Wallaby-Zenith Fracture Zone to the south (Weston et al., 2021). *Alicellea gigantea* is known to be present at abyssal depths of the Wallaby-Zenith Fracture Zone, and this study extends its already expansive multi-oceanic distribution into the hadal depths of the Indian Ocean (Jamieson et al., 2013; Weston et al., 2021). The predatory amphipods of the genus *Princaxelia*, while seemingly rare, are recorded elsewhere at hadal depths (Jamieson et al., 2012b), and this study also extends their distribution to the Indian Ocean. The Stegocephalidae amphipod is the first record of it visiting a baited lander deployed at hadal depths. These individuals were large, similar in length to *B. schellenbergi* or *Eurythenes* spp., however, they had a different and distinctive swimming pattern. One noticeable absence to the hadal amphipod community were *Hirondellea* spp., however, no species of this genus were found at the Wallaby-Zenith Fracture Zone (Weston et al., 2021), thus suggesting a curious absence from hadal depths of the Indian Ocean.

By collating all known records of hadal fauna from the Java Trench with the records from this study (**Supplementary Table 1**), the trench community is now represented by 10 phyla,

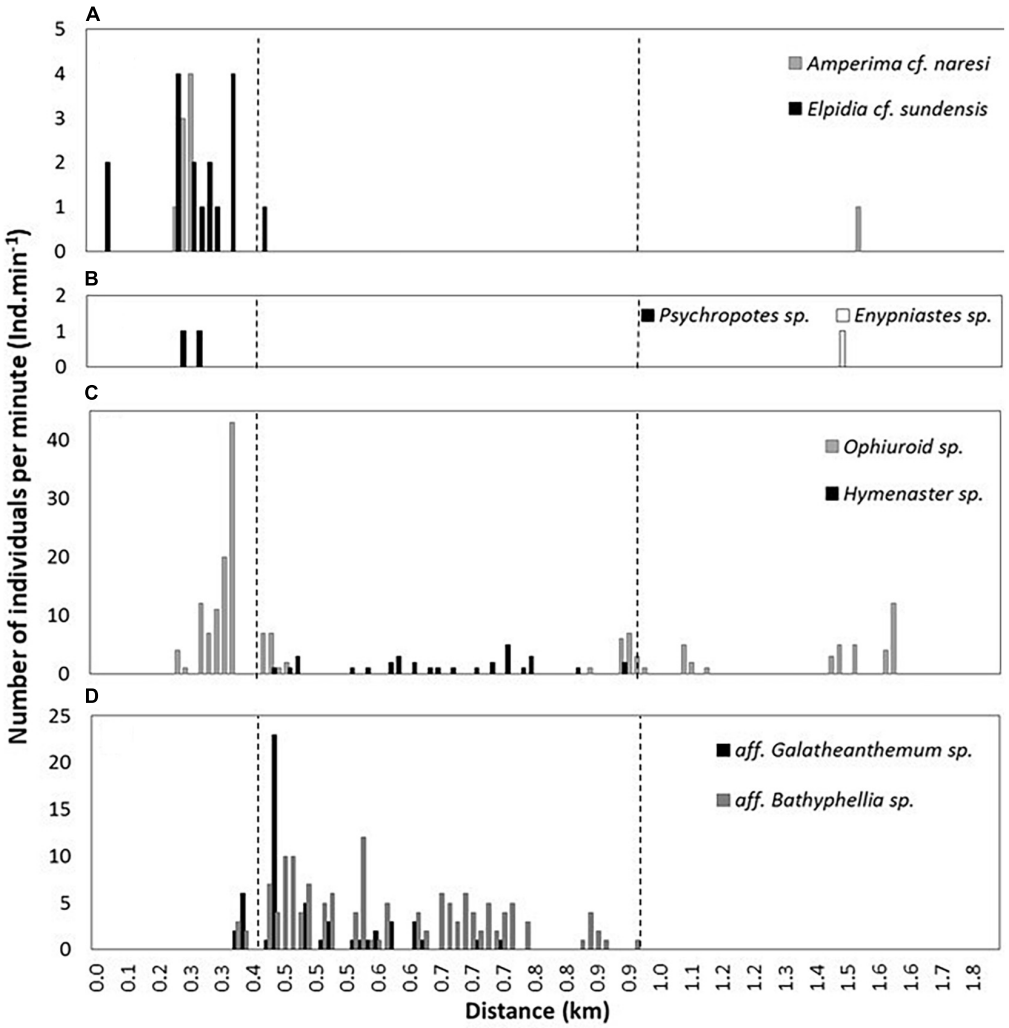

FIGURE 10 | Distribution of epifaunal species. **(A,B)** The four holothurian species. **(C)** The brittle star (*Ophiuroid* sp.) and sea star (*Hymenaster* sp.). **(D)** The actiniarians. The dashed lines represent the start and end of near-vertical slope of the forearc.

21 classes, 34 orders and 55 families. The exact number of genera and species is more difficult to resolve as the two main sources of data are video-derived from this study and from trawl samples taken nearly six decades earlier, many of which were not identified to species level. Thus, there are little visual records of the specimens in which to compare. There are, however, 78 records of > 70 putative species. Of these records, 27% were derived from this study, and 44% if combined with the other published results from the same 5-day expedition (Jamieson and Vecchione, 2020; Jamieson et al., 2021; Jamieson and Linley, 2021; Swan et al., 2021).

Habitat Heterogeneity and Species Distribution

There are two observable patterns relating to the species distribution and the heterogeneity of habitats. The sudden, rather drastic shift between the flat and soft fine-grained sediments of the trench floor to the harder, more complex and steeper sides of the slope resulted in a sudden shift between the holothurian and ophiuroid community on the trench floor to one comprised of actiniarians and asteroids on the slopes (**Figure 10**). On the flatter and relatively soft plateau, the benthic community returns to the former, albeit in fewer numbers. Indeed, the observable numbers of holothurians are greater at the trench floor than on the plateau, and the numbers of actiniarians also increases toward the base of the slope, suggesting better feeding conditions toward the deeper trench floor. The presence of fine-grained sediment with apparent low shear strength, appearing 'softer' with depth, as visually observed by the hadal-landers (**Figure 4**), and between the plateau and trench axis, as observed by the submersible, are thought to be typical of trench settings as seismic and gravitational forces redistribute sediment toward the trench axis (Oguri et al., 2013; Ichino et al., 2015). This sediment transport process is called "trench resource accumulation depth" (TRAD; Jamieson et al., 2010), and thought

to redistribute particulate organic matter by drawing from the upper slopes and accumulating toward the trench axis, thus it coincides with the deepest point of a given trench, regardless of actual depth.

The Java Trench is a comparatively shallow subduction trench (defined as < 8,000 m, Stewart and Jamieson, 2018), which provides the opportunity to compare fauna distribution patterns based on the TRAD. In the Java Trench, the TRAD coincides with groups that are bio-chemically limited to depths < 8,000 m, such as the ophiuroids and asteroids, that are typically absent from the TRADs of deeper trenches (e.g., the Mariana Trench; Jamieson, 2015). In this setting, ophiuroids and asteroids were observed in relatively high numbers compared to other similar studies, such as the Puerto Rico Trench (Jamieson et al., 2020), where they may be opportunistically exploiting the shallower TRAD (**Figure 9**). The high densities of ophiuroids may also be elevated by the unsuitable habitats on the steep escarpment that may be limiting their distribution up the forearc. Conversely, the complex talus deposits of the forearc were utilized by the asteroids and two species of actiniarians. Given the pronounced presence of actiniaria and asteroids on the harder substrates, we hypothesize that on the opposite slope (the underriding plate), where there is generally a thicker sediment drape and perhaps fewer areas of bedrock outcrop present on the subducting abyssal plain, these species are likely to be either absent or far less abundant.

Habitat heterogeneity drives the distribution of species, and in the Java Trench there may be contrasting species diversity and biomass depending on whether the underriding or overriding flank of the trench is being assessed, regardless of water depth. Furthermore, the dense aggregation of hexactinellid sponges underneath the overhang highlights how the habitat heterogeneity influences patchy species distribution. This example of habitat heterogeneity coupled with the complex substrate, three-dimensional structure, and topography observed in this study could only have been realized using a hadal-rated exploratory vehicle and not with free-falling vehicles or towed sampling gear.

Evidence of Chemosynthetic Bacterial Mats

Perhaps the most significant finding from this study is the visual record of the vertical to near vertical bend-related fault escarpment on the forearc. The observations of the putative chemosynthetic bacterial mats on this steep slope show how prevalent and significant this phenomenon might be along all forearc settings, as suggested by Blankenship-Williams and Levin (2009). Interestingly, here we observed 36 bacterial mats in what is estimated to be a 500 m long survey track of a 150 m high portion of the deepest fault escarpment in this trench (**Figures 5B**, **7**). Chemosynthetic communities are typically used as indicators of fluid flow, and their tentative association with structural weaknesses in the bedrock mass reported here, are suggestive of fluid discharge exploiting these pathways. Whether these bacterial mats also occur on more benign sections of the forearc or are limited to these structurally complex escarpments remains unresolved.

In the absence of targeted sediment cores, we are unable to confirm the presence of metazoan organisms associated with the observed chemosynthetic deposits, it is simply more accurate to state that there were no associated organisms visible to the camera. Nonetheless, listed within the trawl specimens from the RV *Vitjaz* expeditions (Belyaev, 1989) were records of Vesicomyidae (Bivalvia), Thyasiridae (Bivalvia), and Siboglinidae (Annelida) which are all typically associated with chemosynthetic deep-sea environments.

The bivalve family Vesicomyidae, are a morphologically diverse, widely distributed, and commonly associated with hydrothermal vents and hydrocarbon seeps (Ruelas-Inzunza et al., 2003; Krylova et al., 2015). Vesicomyidae are also common at abyssal and hadal depths (Knudsen, 1970; Belyaev, 1989). Their association with chemosynthesis was, however, recently questioned by Krylova et al. (2018) who did not detect chemosynthetically fixed carbon in the *Vesicomya* species nor evidence of symbiotic lifestyles, but found that *Vesicomya* possesses a functional gut that is often filled with detritus-like particles, more indicative of detritivory. Indeed, Belyaev (1989) noticed a prevalence of Vesicomyidae in locations near constant coastal derived organic matter suspended in the near-bottom waters, a trend also indicated by Krylova and Sahling (2010), therefore the presence of Vesicomyidae are likely not indicative of chemosynthesis. The family Thyasiridae is also known from vents, seeps and locations associated with organic enrichment (Keuning et al., 2011) and several species are nutritionally dependent on chemoautotrophic bacteria (Dando and Spiro, 1993). Likewise, *Sclerolinum*, a small genus of Siboglinidae, has an obligate mutualistic association with thiotrophic (sulfur-oxidizing) bacteria (Eichinger et al., 2013). The *Sclerolinum* genus is known from many deep-sea settings, found living either on decaying organic materials like sunken wood and sulfidic sediments (Ivanov and Selivanova, 1992; Smirnov, 2000) or hydrothermal vents and cold seeps (Lazar et al., 2010; Pedersen et al., 2010). Thus, it is not surprising to have records of these families in the Java Trench given the high surface primary production, and the presence of wood debris found in this study with the apparent abundance of bacterial mats likely associated with sulfur and other elements.

While this study provides a visual indication of an abundance of potentially chemosynthetic bacterial mats, and the sample records from the RV *Vityaz* expeditions provide an indication of multiple chemosynthetic-associated species, it does appear likely that chemosynthesis may be prevalent in the Java Trench. This adds support to the hypotheses of Blankenship-Williams and Levin (2009) and Hand et al. (2020) that this phenomenon may occur in all or most trenches and may be a key part of the hadal food web, as indicated by Tokuda et al. (2020). The next steps would be to return with the submersible to survey a greater area of seafloor on a variety of geomorphological and geological features with varyingly complex topographies to assess the prevalence of these putative chemosynthetic communities. Direct sampling of these deposits for chemical characterization and epifaunal collection for food web modeling would also be

required to establish the significance of chemosynthesis in the Java Trench, and ultimately its prevalence in hadal ecosystems.

Sampling at hadal depths is typically limited to free fall landers positioned statically on relatively flat seafloor, or historically, trawling that typically targets large areas of relatively flat unobstructed seafloor. The submersible transect, notwithstanding limitations in space and time, provided unexpected insight into how the habitat can rapidly change over a comparatively small distance and in turn alter the benthic biodiversity. By introducing this new technology to these largely unexplored depths within an ocean with a historical paucity of deep-sea research, it was perhaps inevitable that this study would produce such a diverse set of discoveries in just 5 days.

In the 70 years between the ground-breaking expeditions of the *Vityaz* and *Galathea* visits to the Java Trench, the Five Deeps Expedition provided the first visual imagery of the hadal benthic fauna across complex topography at the deepest point of the Indian Ocean. Therein, we recorded multiple new depth and geographical distribution records spanning several taxa, as well as very rare observations such as the first hadal cephalopod, the stalked ascidian and the colony of hexactinellid sponges recessed into the forearc. Furthermore, structural weaknesses in the bedrock mass, that result in repeated rock slope failure and development of extensive talus deposits, appear to also form permeable conduits for fluid discharge that support putative chemosynthetic communities. Being able to freely explore such complex terrain and observe the distribution of species in relation to habitat type provides valuable insight into the natural order of the hadal ecosystem. This in turn can steer the first steps toward more hypothesis driven, and less exploratory driven, science at full ocean depth via targeted sampling with the submersible. These next steps should also bridge the gap between this type of observational research and the taxonomic work derived from the 1950s trawl campaigns (coupled with modern molecular taxonomy), to lift the quality of research from the hadal zone closer to that of its shallower counterparts.

DATA AVAILABILITY STATEMENT

The raw data supporting the conclusions of this article will be made available by the authors, without undue reservation.

AUTHOR CONTRIBUTIONS

AJ contributed to conceptualization. AJ, HS, JW, PL, and VV contributed to investigation: AJ, HS, and JW contributed to resources: AJ and HS contributed to writing—original draft. JW contributed to writing—review and editing. PL and VV contributed to funding acquisition. PL, VV, and AJ participated on the Five Deeps Expedition to the Java Trench in 2019. PL piloted the submersible, while AJ participated as scientific observer, and deployed the baited camera landers, and devised the study. AJ and HS wrote the original draft with JW reviewing and editing the text. All authors conducted the data analysis.

FUNDING

This work was funded by the Caladan Oceanic LLC (US) as part of the Five Deep Expedition. Expedition participation of AJ was supported by Newcastle University's Research Infrastructure Fund (RiF), Exploration of Extreme Ocean Environments. HS was supported by the British Geological Survey Trench Connection project. Open access publication fees were supported by the Minderoo-UWA Deep-Sea Research Centre.

ACKNOWLEDGMENTS

We thank all at Caladan Oceanic LLC (US) and Rob McCallum and Karen Horlick of EYOS Expeditions (US) for their support and logistics, Captain Stuart Buckle and his crew of the DSSV *Pressure Drop* for the safe operations at sea, all at Triton Submarines (US) especially Shane Eigler for his assistance in lander operations, and hydrographic surveyor Cassie Bongiovanni for acquisition of all multibeam echosounder data. We thank Dhugal Lindsay at JAMSTEC and Thomas Linley at Armatus Oceanic for taxonomic assistance.

SUPPLEMENTARY MATERIAL

The Supplementary Material for this article can be found online at: https://www.frontiersin.org/articles/10.3389/fmars.2022.856992/full#supplementary-material

REFERENCES

Belyaev, G. M. (1989). *Deep-Sea Ocean Trenches and Their Fauna*. Moscow: Nauka publishing house.

Birstein, Y. A., and Vinogradov, M. E. (1958). Pelagicheskie gammaridy (*Amphipoda, Gammaridea*) severo-zapadnoi chasti Tikhogo Okeana. [Pelagic Gammaridea from the northwestern Pacific ocean]. *Trudy Instituta Okeanologii Akademija Nauk S.S.S.R.* 27, 219–257.

Blankenship-Williams, L. E., and Levin, L. A. (2009). Living deep: a synopsis of hadal trench ecology. *Mar. Technol. Soc. J.* 43, 137–143. doi: 10.4031/mtsj.43.5.23

Bongiovanni, C., Stewart, H. A., and Jamieson, A. J. (2021). High-resolution multibeam sonar bathymetry of the deepest place in each ocean. *Geosci. Data J.* 00, 1–16.

Chevreux, E. (1899). Sur deux especes geantes d'amphipodes provenant des campagnes du yacht Princesse Alice. *Bull. Zool. Soc. France* 24, 152–158.

Dando, P. R., and Spiro, B. (1993). Varying nutritional dependence of the thyasirid bivalves *Thyasira sarsi* and *T. equalis* on chemoautotrophic symbiotic bacteria, demonstrated by isotope ratios of tissue carbon and shell carbonate. *Mar. Ecol. Prog. Ser.* 92:151. doi: 10.3354/meps092151

Daniell, J., Jorgensen, D. C., Anderson, T., Borissova, I., Burq, S., Heap, A., et al. (2010). Frontier basins of the West Australian continental margin: post-survey report of marine reconnaissance and geological sampling survey GA2476. *Geosci. Aust. Rec.* 2009/38, 1–216.

DeMets, C., Gordon, R. G., and Argus, D. F. (2010). Geologically current plate motions. *Geophys. J. Int.* 181, 1–80.

Eakins, B. W., and Sharman, G. F. (2020). *Volumes of the World's Oceans from ETOPO1*. Boulder, CO: NOAA National Geophysical Data Center.

Eichinger, I., Hourdez, S., and Bright, M. (2013). Morphology, microanatomy and sequence data of *Sclerolinum contortum (Siboglindae. Annelida) of the Gulf of Mexico*. *Org. Divers. Evol.* 13, 311–329. doi: 10.1007/s13127-012-0121-3

Fujikura, K., Kojima, S., Tamaki, K., Maki, Y., Hunt, J., and Okutani, T. (1999). The deepest chemosynthesis-based community yet discovered from the hadal zone, 7326 m deep, in the Japan Trench. *Mar. Ecol. Prog. Ser.* 190, 17–26. doi: 10.3354/meps190017

Fujiwara, Y., Kato, C., Masui, N., Fujikura, K., and Kojima, S. (2001). Dual symbiosis in the cold-seep thyasirid clam *Maorithyas hadalis* from the hadal zone in the Japan Trench, western Pacific. *Mar. Ecol. Prog. Ser.* 214, 151–159.

GEBCO Compilation Group (2021). *GEBCO 2021 Grid* . Available online at: www.gebco.net/data_and_products/gridded_bathymetry_data/ (accessed November 1, 2021).

Hand, K. P., Bartlett, D. H., Fryer, P., Peoples, L., Williford, K., Hofmann, A. E., et al. (2020). Discovery of novel structures at 10.7 km depth in the Mariana Trench may reveal chemolithoautotrophic microbial communities. *Deep Sea Res. 1 Oceanogr. Res. Pap.* 160:103238. doi: 10.1016/j.dsr.2020.103238

Hansen, B. (1956). Holothurioidea from depths exceeding 6000 meters. *Galathea Rep.* 2, 33–54.

Harris, P. T., Macmillan-Lawler, M., Rupp, J., and Baker, E. K. (2014). Geomorphology of the oceans. *Mar. Geol.* 352, 4–24. doi: 10.1098/rsta.2012.0395

Ichino, M. C., Clark, M. R., Drazen, J. C., Jamieson, A. J., Jones, D. O. B., Martin, A. P., et al. (2015). The distribution of benthic biomass in hadal trenches: a modelling approach to investigate the effect of vertical and lateral organic matter transport to the seafloor. *Deep Sea Res. 1 Oceanogr. Res. Pap* 100, 21–33. doi: 10.1016/j.dsr.2015.01.010

Ivanov, A. V., and Selivanova, R. V. (1992). *Sclerolinum javanicum* sp.n., a new pogonophoran living on rotten wood. A contribution to the classification of *Pogonophora*. *Biol. Morya* 1–2, 27–33.

Jamieson, A. J. (2015). *The Hadal zone: Life In The Deepest Oceans*. Cambridge: Cambridge University Press.

Jamieson, A. J. (2020). The five deeps expedition and an update of full ocean depth exploration and explorers. *Mar. Technol. Soc. J.* 54, 6–12. doi: 10.4031/mtsj.54.1.1

Jamieson, A. J., and Linley, T. L. (2021). Hydrozoans, scyphozoans, larvaceans and ctenophores observed in situ at hadal depths. *J. Plankton Res.* 43, 1–13. doi: 10.1093/plankt/fbaa062

Jamieson, A. J., and Vecchione, M. (2020). First in situ observation of Cephalopoda at hadal depths *(Octopoda: Opisthoteuthidae: Grimpoteuthis sp.)*. *Mar. Biol.* 167:82.

Jamieson, A. J., Fujii, T., and Priede, I. G. (2012a). Locomotory activity and feeding strategy of the hadal munnopsid isopod *Rectisura* cf. *herculea (Crustacea: Asellota)* in the Japan Trench. *J. Exp. Biol.* 215, 3010–3017. doi: 10.1242/jeb.067025

Jamieson, A. J., Lörz, A.-N., Fujii, T., and Priede, I. G. (2012b). In situ observations of trophic behaviour and locomotion of *Princaxelia amphipods (Crustacea. Pardaliscidae)* at hadal depths in four West Pacific Trenches. *J. Mar. Biol. Assoc. U.K.* 91, 143–150. doi: 10.1017/s0025315411000452

Jamieson, A. J., Fujii, T., Mayor, D. J., Solan, M., and Priede, I. G. (2010). Hadal trenches: the ecology of the deepest places on earth. *Trends Ecol. Evol.* 25, 190–197. doi: 10.1016/j.tree.2009.09.009

Jamieson, A. J., Gebruk, A., Fujii, T., and Solan, M. (2011). Functional effects of the hadal sea cucumber *Elpidia atakama (Holothuroidea. Elasipodida)* reflect small scale patterns of resource availability. *Mar. Biol.* 158, 2695–2703. doi: 10.1007/s00227-011-1767-7

Jamieson, A. J., Lacey, N. C., Lörz, A.-N., Rowden, A. A., and Piertney, S. B. (2013). The supergiant amphipod *Alicella gigantea (Crustacea: Alicellidae)* from hadal depths in the Kermadec Trench, SW Pacific Ocean. *Deep Sea Res. 2.* 92, 107–113. doi: 10.1016/j.dsr2.2012.12.002

Jamieson, A. J., Linley, T. D., Eigler, S. J., and Macdonald, T. (2021). A global assessment of fishes at lower abyssal and upper hadal depths (5000 to 8000 m). *Deep Sea Res. 1* 178:103642.

Jamieson, A. J., Linley, T. D., Stewart, H. A., Nargeolet, P.-H., and Vescovo, V. (2020). Revisiting the 1964 *Archimède* bathyscaphe dive to 7300 m in the Puerto Rico Trench, abund;ance of an elasipodid holothurian *Peniagone* sp. and a resolution to the identity of the 'Puerto Rican snailfish'. *Deep Sea Res. 1* 162:103336.

Jamieson, A. J., Ramsey, J., and Lahey, P. (2019). Hadal manned submersible. *Sea Technol.* 60, 22–24.

Janßen, F., Treude, T., and Witte, U. (2000). Scavenger assemblages under differing trophic conditions: a case study in the deep Arabian Sea. *Deep Sea Res. 2* 47, 2999–3026. doi: 10.1016/s0967-0645(00)00056-4

Keuning, R., Schander, C., Kongsrud, J. A., and Willassen, E. (2011). Ecology of twelve species of *Thyasiridae (Mollusca: Bivalvia)*. *Mar. Pollut. Bull.* 62, 786–791. doi: 10.1016/j.marpolbul.2011.01.004

Knudsen, J. (1970). The systematics and biology of abyssal and hadal Bivalvia. *Galathea Rep.* 11, 12–41.

Krylova, E. M., and Sahling, H. (2010). Vesicomyidae (*Bivalvia*): current taxonomy and distribution. *PLoS One* 5:e9957. doi: 10.1371/journal.pone.0009957

Krylova, E. M., Kamenev, G. M., Vladychenskaya, I. P., and Petrov, N. B. (2015). Vesicomyinae (*Bivalvia: Vesicomyidae*) of the Kuril–Kamchatka Trench and adjacent abyssal regions. *Deep Sea Res. 2* 111, 198–209. doi: 10.1016/j.dsr2.2014.10.004

Krylova, E. M., Sahling, H., and Borowski, C. (2018). Resolving the status of the families *Vesicomyidae and Kelliellidae (Bivalvia: Venerida)*, with notes on their ecology. *J. Molluscan Stud.* 84, 69–91. doi: 10.1093/mollus/eyx050

Lacey, N. C., Mayor, D. L., Linley, T. D., and Jamieson, A. J. (2018). Population structure of the hadal amphipod *Bathycallisoma (Scopelocheirus) schellenbergi* (*Birstein and Vinogradov*, 1958) in the Kermadec trench and new hebrides trench. SW Pacific. *Deep Sea Res. 2* 155, 50–60. doi: 10.1016/j.dsr2.2017.05.001

Lazar, C., Dinasquet, J., Pignet, P., Prieur, D., and Toffin, L. (2010). Active archaeal communities at cold seep sediments populated by *Siboglinidae* tubeworms from the Storegga Slide. *Microb. Ecol.* 60, 516–527. doi: 10.1007/s00248-010-9654-1

Longhurst, A. (2007). *Ecological Geography of the Sea*, 2nd Edn. San Diego, CA: Academic Press.

McClanahan, T. R., and Muthiga, N. A. (2016). Similar impacts of fishing and environmental stress on calcifying organisms in Indian Ocean coral reefs. *Mar. Ecol. Prog. Ser.* 560, 87–103. doi: 10.3354/meps11921

Oguri, K., Kawamura, K., Sakaguchi, A., Toyofuku, T., Kasaya, T., Murayama, M., et al. (2013). Hadal disturbance in the Japan Trench induced by the 2011 Tohoku–Oki Earthquake. *Sci. Rep.* 3:1915. doi: 10.1038/srep01915

Ohara, Y., Reagan, M. K., Fujikura, K., Watanabe, H., Michibayashi, K., Ishii, T., et al. (2012). A serpentinite-hosted ecosystem in the Southern Mariana Forearc. *Proc. Natl. Acad. Sci.* 109, 2831–2835. doi: 10.1073/pnas.1112005109

Oji, T., Ogawa, Y., Hunter, A. W., and Kitazawa, K. (2009). Discovery of dense aggregations of stalked crinoids in Izu-Ogasawara Trench, Japan. *Zool. Sci.* 26, 406–408. doi: 10.2108/zsj.26.406

Okumura, T., Ohara, Y., Stern, R. J., Yamanaka, T., Onishi, Y., Watanabe, H., et al. (2016). Brucite chimney formation and carbonate alteration at the Shinkai Seep Field, a serpentinite-hosted vent system in the southern Mariana forearc. *Geochem. Geophys. Geosyst.* 17, 3775–3796. doi: 10.1002/2016gc006449

Omura, A., Ikehara, K., and Arai, K. (2017). Determining sources of deep-sea mud by organic matter signatures in the Sunda trench and Aceh basin off Sumatra. *Geo Mar. Lett.* 37, 549–559. doi: 10.1007/s00367-017-0510-x

Parulekar, A. H., Harkantra, S. N., Ansari, Z. A., and Matondkar, S. G. P. (1982). Abyssal benthos of the central Indian Ocean. *Deep Sea Res. Part A* 29, 1531–1537.

Paterson, G. L., Glover, A. G., Froján, C. R. B., Whitaker, A., Budaeva, N., Chimonides, J., et al. (2009). A census of abyssal polychaetes. *Deep Sea Res. 2* 56, 1739–1746. doi: 10.1016/j.dsr2.2009.05.018

Pavithran, S., Ingole, B. S., Nanajkar, M., Raghukumar, C., Nath, B. N., and Valsangkar, A. B. (2009). Composition of macrobenthos from the central Indian Ocean Basin. *J. Earth Syst. Sci.* 118:689. doi: 10.11646/zootaxa.4878.3.2

Pedersen, R. B., Rapp, H. T., Thorseth, I. H., Lilley, M. D., Barriga, F. J., Baumberger, T., et al. (2010). Discovery of a black smoker vent field and vent fauna at the Arctic Mid-Ocean Ridge. *Nat. Commun.* 1, 1–6. doi: 10.1038/ncomms1124

Picard, K., Brooke, B. P., Harris, P. T., Siwabessy, P. J., Coffin, M. F., Tran, M., et al. (2018). Malaysia Airlines flight MH370 search data reveal geomorphology and seafloor processes in the remote southeast Indian Ocean. *Mar. Geol.* 395, 301–319. doi: 10.1016/j.margeo.2017.10.014

Rogers, A. (2016). Pelagic ecology of the South West Indian Ocean Ridge seamounts: introduction and overview. *Deep Sea Res. 3* 136:9. doi: 10.1016/j.dsr2.2016.12.009

Rogers, A. D., Alvheim, O., Bemanaja, E., Benivary, D., Boersch-Supan, P., Bornman, T. G., et al. (2017). Pelagic communities of the South West Indian Ocean seamounts: R/V Dr Fridtjof Nansen Cruise. 2009–2410. *Deep Sea Res. 2*, 136, 5–35. doi: 10.1016/j.dsr2.2016.12.010

Ruelas-Inzunza, J., Soto, L. A., and Páez-Osuna, F. (2003). Heavy-metal accumulation in the hydrothermal vent clam *Vesicomya gigas* from Guaymas basin. Gulf of California. *Deep Sea Research 1* 50, 757–761. doi: 10.1016/s0967-0637(03)00054-2

Sheppard, C. R. (1998). Biodiversity patterns in Indian Ocean corals, and effects of taxonomic error in data. *Biodivers. Conserv.* 7, 847–868. doi: 10.1023/a:1008830222860

Smirnov, R. V. (2000). Two new species of *Pogonophora* from the arctic mud volcano off northwestern Norway. *Sarsia* 85, 141–150. doi: 10.1080/00364827.2000.10414563

Smith, W. H., and Marks, K. M. (2014). Seafloor in the Malaysia Airlines flight MH370 search area. *Eos* 95, 173–174. doi: 10.1002/2014eo210001

Stefanoudis, P., Talma, S., Samimi-Namin, K., and Woodall, L. (2020). Deep reef ecosystems of the Western Indian Ocean: addressing the great unknown. *Res. Ideas Outcomes* 6:e53913.

Stewart, H. A., and Jamieson, A. J. (2018). Habitat heterogeneity of hadal trenches: considerations and implications for future studies. *Prog. Oceanogr.* 161, 47–65.

Stewart, H. A., and Jamieson, A. J. (2019). The five deeps: the location and depth of the deepest place in each of the world's oceans. *Earth Sci. Rev.* 197:102896. doi: 10.1016/j.earscirev.2019.102896

Swan, J. A., Jamieson, A. J., Linley, T. L., and Yancey, P. Y. (2021). Worldwide distribution and depth limits of decapod crustaceans (*Penaeoidea. Oplophoroidea)* across the abyssal-hadal transition zone of eleven subduction trenches and five additional deep-sea features. *J. Crust. Biol.* 41:ruaa102.

Théel, H. (1882). Report on the Holothuroidea dredged by H.M.S. 'Challenger' during the years 1873-76. Part i. Report on the Scientific Results of the Voyage of H.M.S. Challenger during the years 1873–1876. *Zoology*. 4(part 13): i–ix, 1–176.

Tokuda, A. K., Drazen, J. C., Gerringer, M. E., Popp, B. N., Grammatopoulou, E., and Mayor, D. J. (2020). Trophic interactions of megafauna in the Mariana and Kermadec trenches inferred from stable isotope analysis. *Deep Sea Res. 1* 164:103360.

Vacelet, J., Boury-Esnault, N., and Harmelin, J. G. (1994). Hexactinellid cave, a unique deep-sea habitat in the scuba zone. *Deep Sea Res. 1* 41, 965–973. doi: 10.1016/0967-0637(94)90013-2

Wafar, M., Venkataraman, K., Ingole, B., Khan, S. A., and LokaBharathi, P. (2011). State of knowledge of coastal and marine biodiversity of Indian Ocean countries. *PLoS One* 6:E14613. doi: 10.1371/journal.pone.0014613

Weston, J. N. J., Peart, R. A., and Jamieson, A. J. (2020). Amphipods from the wallaby-zenith fracture zone, Indian Ocean: new genus and two new species identified by integrative taxonomy. *Syst. Biodivers.* 18, 57–78.

Weston, J. N. J., Peart, R. A., Stewart, H. A., Ritchie, H., Piertney, S. B., Linley, T. D., et al. (2021). Scavenging amphipods from the wallaby-zenith fracture zone: extending the hadal paradigm beyond subduction trenches. *Mar. Biol.* 68, 1–14.

Wolff, G. A., Billett, D. S. M., Bett, B. J., Holtvoeth, J., FitzGeorge-Balfour, T., Fisher, E. H., et al. (2011). The effects of natural iron fertilisation on deep-sea ecology: the crozet plateau, Southern Indian Ocean. *PLoS One* 6:e20697. doi: 10.1371/journal.pone.0020697

Wolff, T. (1960). The hadal community, an introduction. *Deep Sea Res.* 6, 95–124. doi: 10.1016/0146-6313(59)90063-2

Wölfl, A. C., Snaith, H., Amirebrahimi, S., Devey, C. W., Dorschel, B., Ferrini, V., et al. (2019). Seafloor Mapping–the challenge of a truly global ocean bathymetry. *Front. Mar. Sci.* 6:283. doi: 10.3389/fmars.2019.00283

Conflict of Interest: PL was employed by the company Triton Submarines LLC. VV was employed by the company Caladan Oceanic LLC.

The remaining authors declare that the research was conducted in the absence of any commercial or financial relationships that could be construed as a potential conflict of interest.

Publisher's Note: All claims expressed in this article are solely those of the authors and do not necessarily represent those of their affiliated organizations, or those of the publisher, the editors and the reviewers. Any product that may be evaluated in this article, or claim that may be made by its manufacturer, is not guaranteed or endorsed by the publisher.